

¹A. SANDHYA, ²G. Venkata Ramana REDDY, ³G.V.S.R. DEEKSHITULU

RADIATION AND CHEMICAL REACTION EFFECTS ON MHD CASSON FLUID FLOW PAST A SEMI-INFINITE VERTICAL MOVING POROUS PLATE

¹.JNTUK Kakinada, Department of Mathematics, VR Siddhartha Engineering College, Kanur, Vijayawada, INDIA².Department of Mathematics, Koneru Lakshmaiah Education Foundation, Vaddeswaram, Guntur, INDIA³.Department of Mathematics, JNTUK Kakinada, INDIA

Abstract: A speculative investigation has been presented to explore the significant features of MHD convective Casson fluid flow past a semi-infinite moving vertical porous plate with heat source/sink are included in the flow configuration. The governing partial differential equations are remodeled into ordinary differential equations using appropriate non-dimensional variables. The ensuing differential equations are solved analytically using two term perturbation technique method. The result of flow heat and mass transfer analysis on the velocity, temperature and concentration profiles are given graphically. The numerical values of the physical parameters like Skin friction, Nusselt number, and Sherwood number are shown in tabular form, results shows that Casson parameter enhances the velocity, temperature and concentration fields are decreases for increasing the values radiation and chemical reaction.

Keywords: Casson parameter, MHD, Heat source/sink, Heat and mass transfer

1. INTRODUCTION

The analysis of non-Newtonian Casson fluid can be described as a shear thinning liquid at zero rate of shear having an infinite viscosity, at an infinite rate of shear, a yield stress below having zero viscosity and no flows occurs. If a yield stress greater than the shear stress is applied to the fluid, it behaves like a solid, where as if a yield stress less than shear stress is applied and it starts to move. Few examples of Casson fluids are tomato sauce, jelly, concentrated fruit juice, honey, blood etc.

Shehzad et al.[1] described the mass transfer effects on MHD Casson fluid flow with chemical reaction. Vajravelu et al. [2] analyzed in flow of the casson fluid dispersal of chemically reactive species over permeable an unsteady stretching surface. Abid et al. [3] discussed unsteady heat transfer and boundary layer flow of a Casson fluid past an oscillating Newtonian heating with vertical plate. Sekhar et al. [4] analyzed convective heat and mass transfer of unsteady MHD Casson fluid past a permeable semi-infinite vertical moving plate with heat source/sink. Animasaun [5] developed effects of thermal conductivity, variable viscosity and thermophoresis on Non-Darcian MHD free convective heat and mass transfer of dissipative Casson fluid flow with nth order of chemical reaction and suction. Suresh et al.[6] studied effect of radiative and dissipative free convective heat transfer flow of a Casson fluid due to variable internal heat generation and thermal conductivity past a stretching sheet. Falodun et al. [7] computed numerically heat transfer on unsteady incompressible magnetohydrodynamic (MHD) boundary layer fluid flow of a vertical moving plate. Falodun[8] studied the effect of thermophoresis on MHD heat and mass transfer flow past of Casson fluid a semi-infinite vertical plate. Makinde et al. [9] discussed the effect of chemical reaction on MHD Casson fluid flow with porous stretching sheet. Rama Krishna Reddy et al. [10] presented Free convective MHD flow past a porous plate. Nagasantoshi [11] studied heat and mass transfer of non-Newtonian flow of Nano fluid over a stretching sheet with non-uniform variable viscosity and heat source. Gvrreddy [12] discussed Soret and Dufour effects on flow of MHD micropolar fluid through a non-Darcy porous medium over a linearly stretching sheet. Suneetha et al. [13] represented effects of heat source and radiation effects on MHD flow through porous stratum over a permeable stretching sheet with chemical reaction. Vijaya et al. [14] developed effects of radiation and Soret on an unsteady Casson fluid flow through vertical porous channel with contraction and expansion. Ramana Reddy et al.[15] represented numerical solutions of unsteady heat transfer MHD flow over a stretching surface with injection or suction.

In view of these an investigation, the major concerns of present pattern are to consider the magnetohydrodynamic convective Casson fluid flow past a semi-infinite vertical moving porous plate with heat source/sink are included in the flow. The mathematical modelling of flow arrangement yields simultaneous non-linear partial differential equations. The appropriate two term perturbation technique method employed to governing equations to deduce two non-dimensional ordinary differential equations. The numerical values of the physical parameters like Skin friction, Nusselt number, and Sherwood number are shown in tabular form.

2. MATHEMATICAL ANALYSIS

We consider an unsteady two-dimensional free convective MHD flow of a viscous, an electrically conducting, heat absorbing and incompressible fluid past a semi-infinite permeable vertical plate insert in a uniform porous medium which having boundary condition at the collaborate of fluid layers and porous medium. A uniform transversal magnetic field of

strength B_0 is applied in the presence of radiation and concentration buoyancy effects in the y' -axis direction. The transversely applied magnetic Reynolds number and magnetic field are considered to be very small so that induced magnetic field and Hall Effect are negligible. It is considered that there is no applied voltage which results the deficiency of electric field. The length of the plate is large enough and the motion is two-dimensional so all the physical variables are independent of x' .

The wall is maintained at constant concentration C_w and temperature T_w , greater than the surrounding concentration C'_∞ and temperature T'_∞ , respectively. Also, it is considered that there exists a first-order homogeneous Casson fluid and the heat source. It is considered to be homogeneous porous and exist everywhere in local thermodynamic equilibrium. Remaining properties of the porous medium and the fluid are taken to be constant. Under these assumptions, the governing equations can be expressed as:

$$\frac{\partial v'}{\partial y'} = 0 \quad (1)$$

$$\frac{\partial u'}{\partial t'} + v' \frac{\partial u'}{\partial y'} = -\frac{1}{\rho} \frac{\partial p'}{\partial x'} + \nu \left(1 + \frac{1}{\beta} \right) \frac{\partial^2 u'}{\partial y'^2} + g \beta_T (T' - T'_\infty) + g \beta_C (C' - C'_\infty) - \frac{\sigma B_0^2}{\rho} u' - \frac{\nu}{k'} u' \quad (2)$$

$$\frac{\partial T'}{\partial t'} + v' \frac{\partial T'}{\partial y'} = \alpha \frac{\partial^2 T'}{\partial y'^2} - \frac{Q_0}{\rho c_p} (T' - T'_\infty) - \frac{1}{\rho c_p} \frac{\partial q_r'}{\partial y'} \quad (3)$$

$$\frac{\partial C'}{\partial t'} + v' \frac{\partial C'}{\partial y'} = D \frac{\partial^2 C'}{\partial y'^2} - Kr (C' - C'_\infty) \quad (4)$$

where x' and y' are the dimensional distances along to the plate. u' and v' are the of dimensional velocity components along x' and y' directions. g is the gravitational acceleration, T' is the fluid dimensional temperature near the plate, T'_∞ is the stream dimensional temperature far away from the plate, C' is the dimensional concentration of the fluid, C'_∞ is the stream dimensional concentration far away from the plate. β_T and β_C - expansion coefficients of the thermal and concentration respectively. p' is the pressure, c_p is the specific heat, B_0 is the coefficient of magnetic field, μ is fluid viscosity, ρ is the density, K is the thermal conductivity, σ is the density of the fluid magnetic permeability, $\nu = \frac{\mu}{\rho}$ is the

kinematic viscosity, D is the diffusivity of the molecular, Q_0 is the dimensional coefficient of the heat absorption and β is the Casson parameter. The third and fourth terms of RHS of Eq. (2) denote the thermal and concentration buoyancy effects, respectively.

$$u' = u'_p, T' = T'_w + \varepsilon (T'_w - T'_\infty) e^{n'y'}, C' = C'_w + \varepsilon (C'_w - C'_\infty) e^{n'y'} \quad \text{at } y' = 0 \quad (5)$$

$$u' = U'_\infty = U_0 (1 + \varepsilon e^{n'y'}), T' \rightarrow T'_\infty, C' \rightarrow C'_\infty \quad \text{as } y' \rightarrow \infty \quad (6)$$

where U'_p , T'_w , C'_w , are the wall dimensional velocity, temperature and concentration, respectively. U'_∞ , T'_∞ , C'_∞ , are the free stream dimensional velocity, temperature and concentration, respectively U_0 , n' are constants.

The radiative flux vector q_r' can be written by using the Rosseland approximation as:

$$q_r' = -\frac{4\sigma^*}{3k'_1} \frac{\partial T_w'^4}{\partial y'} \quad (7)$$

where, σ^* and k'_1 are the Stefan-Boltzmann constant and mean absorption coefficient respectively. We considered that the temperature difference is sufficiently small within the flow such that $T_w'^4$ can be represented as a linear function of the temperature. This is obtained by expanding in a Taylor series neglecting higher order terms about the free stream temperature T'_∞ , thus

$$T_w'^4 \cong 4T_\infty'^3 T'_w - 3T_\infty'^4 \quad (8)$$

From Eq.(1) the velocity of the suction at the plate surface is a function of time only. Assuming that it takes exponential form as follows:

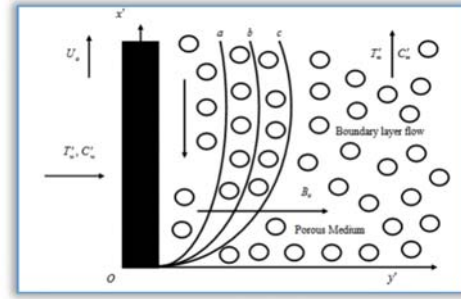


Figure 1. Physical configuration of the problem

$$v' = -V_0(1 + \varepsilon A e^{nt'}) \quad (9)$$

where V_0 is a scale of suction velocity which has non-zero positive constant, A is a real positive constant and ε and εA are small less than unity. Eq. (2) gives the Outside boundary layer

$$-\frac{1}{\rho} \frac{dp'}{dx'} = \frac{dU'_\infty}{dt'} + \frac{\sigma}{\rho} B_0^2 U'_\infty + \frac{\nu}{K'} U'_\infty \quad (10)$$

Let us introducing the non-dimensional quantities

$$\begin{aligned} u &= \frac{u'}{V_0}, v = \frac{v'}{V_0}, y = \frac{V_0 y'}{\nu}, U_\infty = \frac{U'_\infty}{U_0}, t = \frac{t' V_0^2}{\nu}, \theta = \frac{T' - T'_\infty}{T'_w - T'_\infty}, \\ \phi &= \frac{C' - C'_\infty}{C'_w - C'_\infty}, U_p = \frac{u'_p}{U_0}, Sc = \frac{\nu}{D}, K = \frac{K' V_0^2}{\nu^2}, Q = \frac{Q_0 \nu}{\rho C_p V_0^2}, \\ M &= \frac{\sigma B_0^2 \nu}{\rho V_0^2}, Gr = \frac{\rho \nu g (T'_w - T'_\infty) \beta_r}{U_0 V_0^2}, Gc = \frac{\rho \nu g (C'_w - C'_\infty) \beta_c}{U_0 V_0^2}, Pr = \frac{\nu C_p}{K} = \frac{\nu}{\alpha} \end{aligned} \quad (11)$$

In the view of the above dimensionless variables, the basic field of Eqs. (2)-(4) can be expressed in non-dimensional form as

$$\frac{\partial u}{\partial t} - (1 + \varepsilon A e^{nt}) \frac{\partial u}{\partial y} = \frac{dU_\infty}{dt} + \frac{\partial^2 u}{\partial y^2} \left(1 + \frac{1}{\beta} \right) + Gr\theta + Gc\phi - N(U_\infty - u) \quad (12)$$

$$\frac{\partial \theta}{\partial t} - (1 + \varepsilon A e^{nt}) \frac{\partial \theta}{\partial y} = \frac{1}{Pr} \frac{\partial^2 \theta}{\partial y^2} - (Q + R)\theta \quad (13)$$

$$\frac{\partial \phi}{\partial t} - (1 + \varepsilon A e^{nt}) \frac{\partial \phi}{\partial y} = \frac{1}{Sc} \frac{\partial^2 \phi}{\partial y^2} - Kr\phi \quad (14)$$

where, $N = \left(M + \frac{1}{K} \right)$

The corresponding boundary conditions (5) and (6) in non-dimensional form are

$$u = U_p, \theta = 1 + \varepsilon e^{nt}, \phi = 1 + \varepsilon e^{nt} \text{ at } y=0 \quad (15)$$

$$u = U_\infty = (1 + \varepsilon e^{nt}), \theta \rightarrow 0, \phi \rightarrow 0 \text{ as } y \rightarrow \infty \quad (16)$$

3. SOLUTION OF THE PROBLEM

Eqs. (12)- (14) represent a set of partial differential equations that cannot be solved in closed-form. However, it can be reduced to a set of ordinary differential equations in dimensionless form that can be solved analytically. This can be done by representing the velocity, temperature and concentration as

$$u(y, t) = u_0(y) + \varepsilon e^{nt} u_1(y) + O(\varepsilon^2) + \dots \quad (17)$$

$$\theta(y, t) = \theta_0(y) + \varepsilon e^{nt} \theta_1(y) + O(\varepsilon^2) + \dots \quad (18)$$

$$\phi(y, t) = \phi_0(y) + \varepsilon e^{nt} \phi_1(y) + O(\varepsilon^2) + \dots \quad (19)$$

Substituting (17)-(19) into Eqs.(12)-(14) and equating the harmonic and non-harmonic terms, and neglecting the higher order $O(\varepsilon^2)$ and simplifying to get the following pairs of equations for u_0, θ_0, ϕ_0 and u_1, θ_1, ϕ_1

$$\left(1 + \frac{1}{\beta} \right) u_0'' + u_0' - Nu_0 = -[Gr\theta_0 + Gc\phi_0 + N] \quad (20)$$

$$\left(1 + \frac{1}{\beta} \right) u_1'' + u_1' - (N + n)u_1 = -[Gr\theta_1 + Gc\phi_1 + Au_0' + N + n] \quad (21)$$

$$\theta_0'' + Pr\theta_0' - (Q + R)Pr\theta_0 = 0 \quad (22)$$

$$\theta_1'' + Pr\theta_1' - (Q + R + n)\theta_1 = -A\theta_0' \quad (23)$$

$$\phi_0'' + Sc\phi_0' - ScKr\phi_0 = 0 \quad (24)$$

$$\phi_1'' + Sc\phi_1' - Sc(Kr + n)\phi_1 = -A\phi_0' \quad (25)$$

Where the prime denotes ordinary differentiation with respect to y ,

The corresponding boundary conditions are

$$u'_0 = u'_p, u'_1 = 1, \theta'_0 = 1, \theta'_1 = 1, \phi'_0 = 1, \phi'_1 = 1 \text{ as } y'=0 \quad (26)$$

$$u'_0 = 1, u'_1 = 1, \theta'_0 \rightarrow 0, \theta'_1 \rightarrow 0, \phi'_0 \rightarrow 0, \phi'_1 \rightarrow 0 \text{ as } y' \rightarrow \infty \quad (27)$$

without going into the details, the solutions of Eqs. (20)-(25) With the help of boundary conditions (26) and (27), we get

$$u_0 = A_7 e^{(-m_5 y)} + A_5 e^{(-m_3 y)} + A_6 e^{(-m_1 y)} + 1 \quad (28)$$

$$u_1 = A_{17} e^{(-m_6 y)} + A_8 e^{(-m_5 y)} + A_{11} e^{(-m_4 y)} + A_{15} e^{(-m_3 y)} + A_{13} e^{(-m_2 y)} + A_{16} e^{(-m_1 y)} + 1 \quad (29)$$

$$\theta_0 = e^{-m_3 y} \quad (30)$$

$$\theta_1 = A_4 e^{-m_4 y} + A_3 e^{-m_3 y} \quad (31)$$

$$\phi_0 = e^{-m_1 y} \quad (32)$$

$$\phi_1 = A_2 e^{-m_2 y} + A_1 e^{-m_1 y} \quad (33)$$

In view of the above solutions, the velocity, temperature and concentration distributions in the boundary layer become

$$u(y, t) = (A_7 e^{(-m_5 y)} + A_5 e^{(-m_3 y)} + A_6 e^{(-m_1 y)} + 1) \quad (34)$$

$$+ \varepsilon e^{nt} (A_{17} e^{(-m_6 y)} + A_8 e^{(-m_5 y)} + A_{11} e^{(-m_4 y)} + A_{15} e^{(-m_3 y)} + A_{13} e^{(-m_2 y)} + A_{16} e^{(-m_1 y)} + 1)$$

$$\theta(y, t) = (e^{-m_3 y}) + \varepsilon e^{nt} (A_4 e^{-m_4 y} + A_3 e^{-m_3 y}) \quad (35)$$

$$\phi(y, t) = (e^{-m_1 y}) + \varepsilon e^{nt} (A_2 e^{-m_2 y} + A_1 e^{-m_1 y}) \quad (36)$$

The Skin-friction coefficient, the Nusselt number and the Sherwood number are significant physical parameters for this type of boundary-layer flow. These parameters can be defined and determined as follows:

4. SKIN FRICTION, NUSSELT NUMBER AND SHERWOOD NUMBER

In the non-dimensional form the skin friction on the plate $y = 0$, after getting the velocity field is given by

$$C_f = \frac{\tau'_w}{\rho U_0 V_0} = \frac{\partial u}{\partial y} \Big|_{y=0} \quad (37)$$

$$= - \left[(m_5 A_7 + m_3 A_5 + m_1 A_6) + \varepsilon e^{nt} (m_6 A_{17} + m_5 A_8 + m_4 A_{11} + m_3 A_{15} + m_2 A_{13} + m_1 A_{16}) \right]$$

The heat transfer coefficient can be obtained by the temperature field, which is in non-dimensional form in terms of Nusselt number is given by

$$Nu = x \frac{\partial \theta}{\partial y'} \Big|_{y=0} \Rightarrow Nu Re_x^{-1} = \frac{\partial \theta}{\partial y} \Big|_{y=0} = \left[m_3 + \varepsilon e^{nt} (m_4 A_4 + m_3 A_3) \right] \quad (38)$$

where $Re_x = \frac{V_0 x}{\nu}$ is the Reynolds number.

The rate of mass transfer coefficients can be obtained with the concentration field, in the non-dimensional form in terms of Sherwood number is given by

$$Sh_x = x \frac{\partial \phi}{\partial y'} \Big|_{y=0} \Rightarrow Sh_x Re_x^{-1} = \frac{\partial \phi}{\partial y} \Big|_{y=0} = - \left[m_1 + \varepsilon e^{nt} (m_2 A_2 + m_1 A_1) \right] \quad (39)$$

5. RESULTS AND DISCUSSION

The system of non-linear coupled ordinary differential equations (12)-(14) having boundary conditions are solved analytically, using two term perturbation techniques. Numerical values obtained for the problem are expressed in terms of graphs for various flow parameters. Impact of magnetic parameter (M), Casson parameter (β), permeability parameter (K), Grashof number (Gr), modified Grashof number (Gc), Prandtl number (Pr), heat source (Q), radiation parameter (R), chemical reaction (Kr) and Schmidt number (Sc) on the velocity, temperature and concentration profiles are discussed.

Figures 2 and 3 represents the velocity profiles for different values of magnetic parameter (M) and permeability parameter (K) for different values respectively. In Figure 2 the velocity profile falls with the raising of magnetic parameter values, due to the presence of a magnetic field in an electrically conducting fluid produced Lorentz force that acts against the flow, if the magnetic field applied in the normal direction as within the study. But the reverses trend is observed, the velocity profiles for increasing values of permeability parameter in Figure 3.

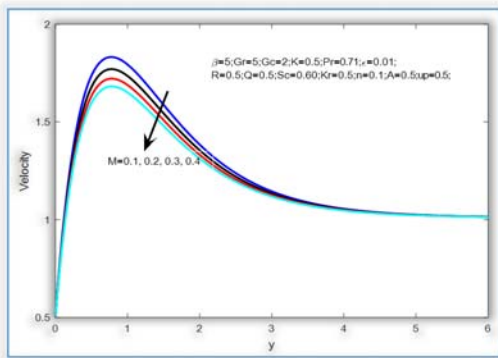


Figure 2. Velocity profiles for different values of magnetic parameter

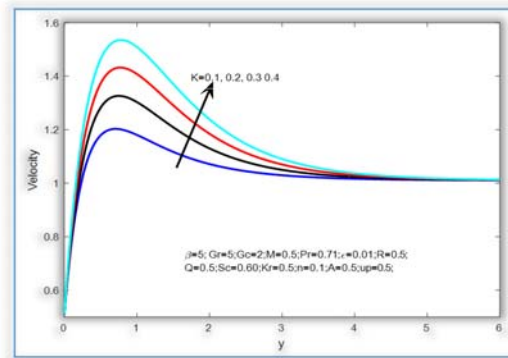


Figure 3. Velocity profiles for different values of permeability parameter

Velocity distribution for various values of Grashof number (Gr) and modified Grashof number (Gc) are represented in Figures 4 and 5 respectively as seen in these figures the maximum peak value is obtained in the absence of buoyancy force, this is because of the buoyancy forces improves the boundary layer thickness and the fluid velocity increases in the increasing the values of the Grashof number and modified Grashof number.

The impact of Prandtl number (Pr) for the temperature and velocity profiles are as shown in the Figures 6 and 7 respectively at the temperature and velocity both are decreases for increasing values of Prandtl number, due to smaller values of Prandtl number are similar to raising the thermal conductivities and so heat is ready to decreases far away from the heated surface for greater values of Prandtl number.

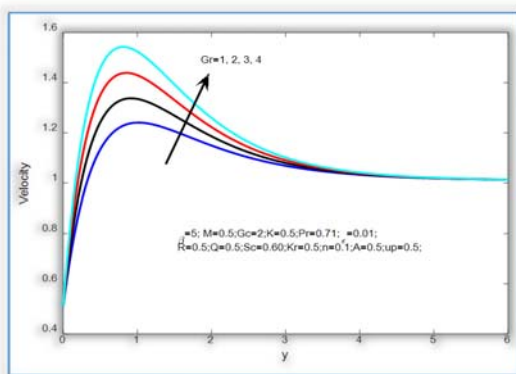


Figure 4. Velocity profiles for different values of Grashof number

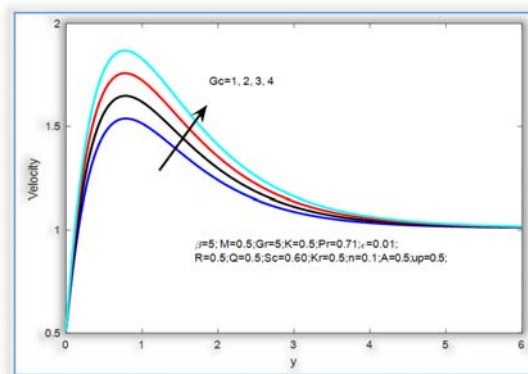


Figure 5. Velocity profiles for different values of modified Grashof number

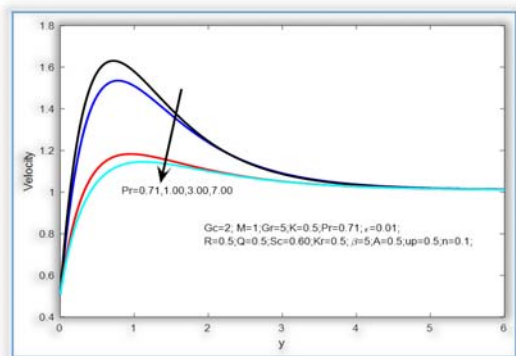


Figure 6. Velocity profiles for different values of Prandtl number

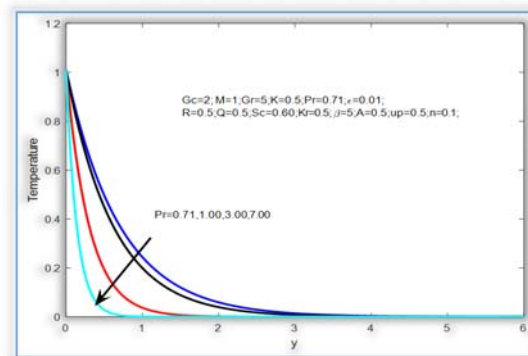


Figure 7. Temperature profiles for different values of Prandtl number

The impact of the Casson parameter (β) and the velocity profiles as shown in the Figure 8 it is observed that the velocity profiles increases for increasing values of Casson fluid parameter. Figures 9 and 10 represent the temperature profiles for various values of heat source/sink parameter (Q), radiation parameter (R) respectively. It is noticed that as the value of heat source and radiation parameters increases, the temperature profiles decreases. Figures 11 and 12 represent the concentration and velocity profiles for various different values of chemical reaction parameter (Kr). It is noticed that both the concentration and velocity profiles are decreases for increasing value of chemical reaction parameter.

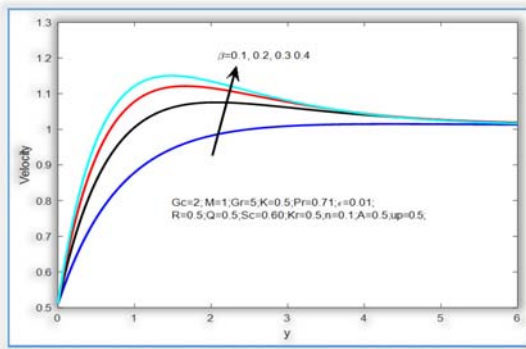


Figure 8. Velocity profiles for different values of Casson parameter

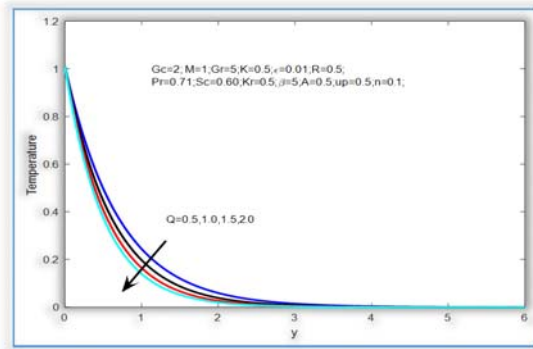


Figure 9. Temperature profiles for different values of heat source parameter

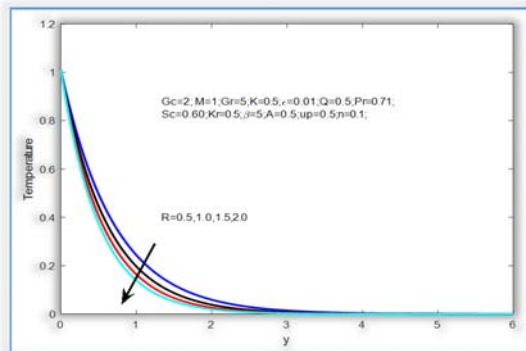


Figure 10. Temperature profiles for different values of radiation parameter

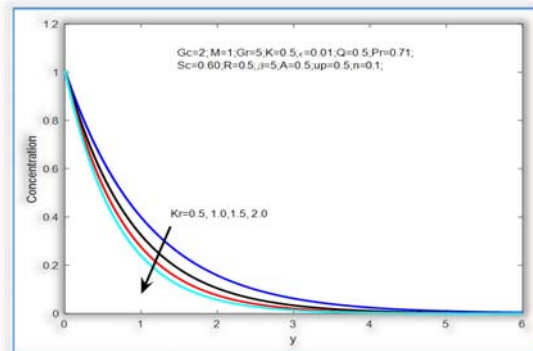


Figure 11. Concentration profiles for different values of Chemical reaction parameter

Figures 13 and 14 exhibit the effect of the velocity and concentration profiles for different values of Schmidt number (Sc).

It is noticed that both the velocity and concentration profiles are decreases for increasing value of Schmidt number. Figure 15 represents the effect of magnetic parameter (M) on the skin friction profiles. It is noticed that the magnetic parameter increases, decrease the skin-friction. Also it is noticed that from the Figures 16, 17 and 19 that the skin-friction coefficient increases for the increased values of radiation parameter (R), permeability parameter (K) and chemical reaction parameter (Kr) respectively. Figures 18 and 20 represent the effect of chemical reaction parameter (Kr) and radiation (R) on the Nusselt number and Sherwood number respectively. It is observed that the Nusselt number and Sherwood number both increases for increasing values radiation and chemical reaction parameter respectively.

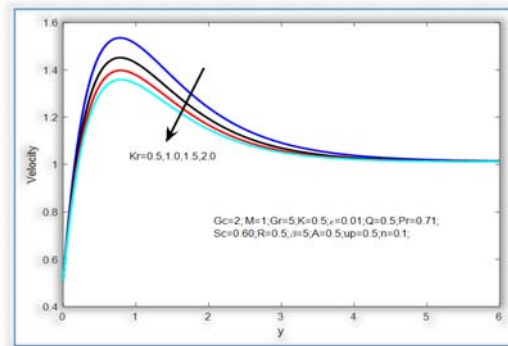


Figure 12. Velocity profiles for different values of Chemical reaction parameter

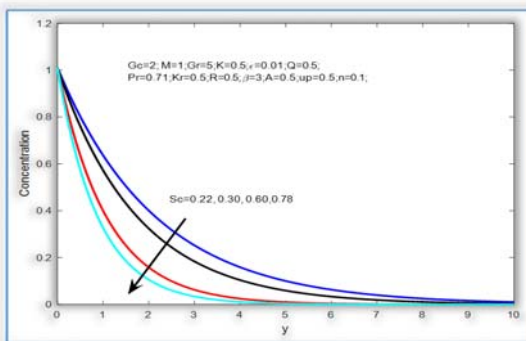


Figure 13. Concentration profiles for different values of Schmidt number

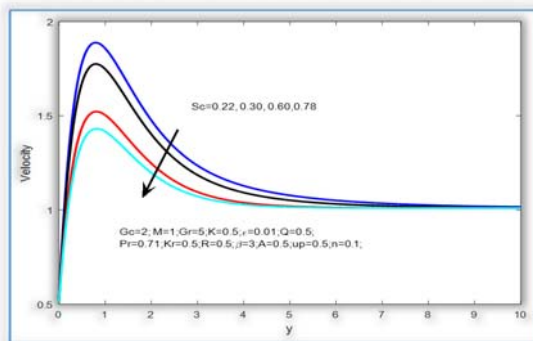


Figure 14. Velocity profiles for different values of Schmidt number

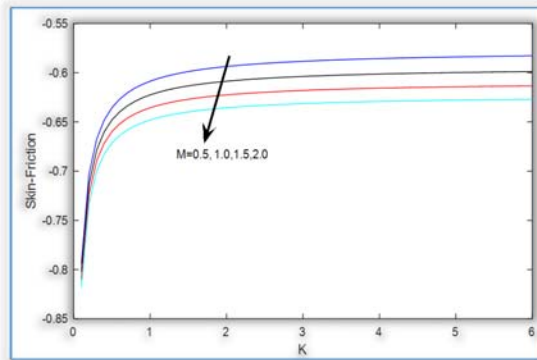


Figure 15. Skin friction coefficient for different values of M with K

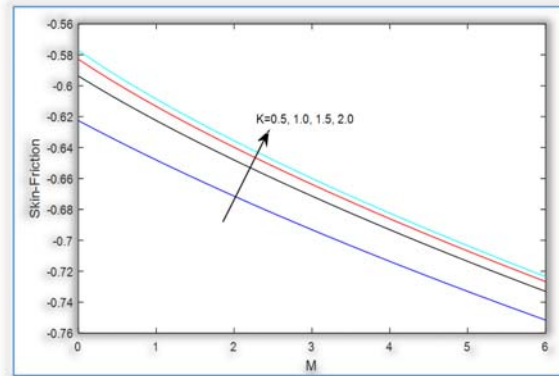


Figure 16. Skin friction coefficient for different values of K with M

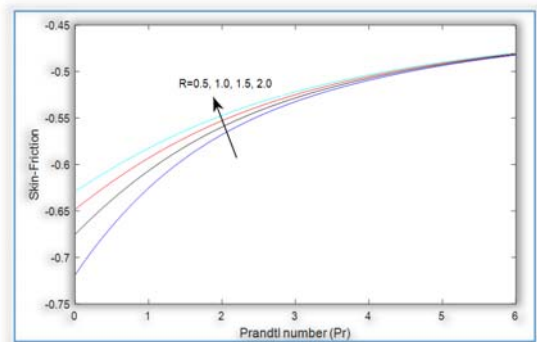


Figure 17. Skin friction coefficient for different values of R with Pr

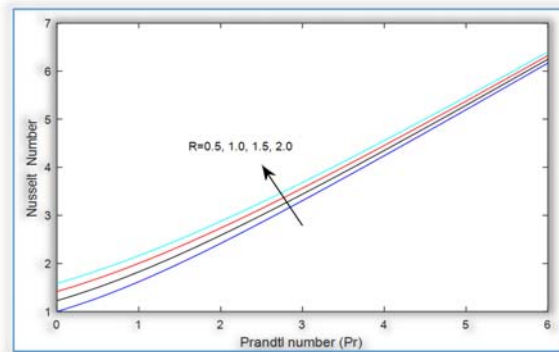


Figure 18. Nusselt number for different values of R with Pr

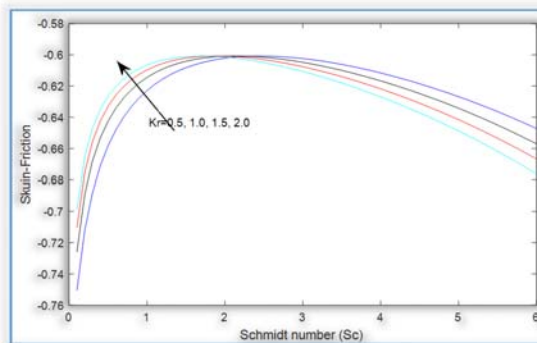


Figure 19. Skin friction coefficient for different values of Kr with Sc

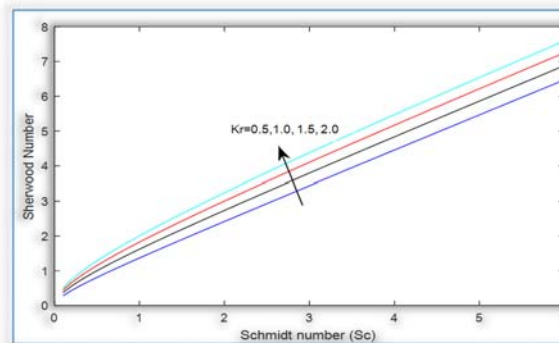


Figure 20. Sherwood number for different values of Kr with Sc

6. CONCLUSIONS

Numerical results for velocity, temperature and concentration profiles are procured for constant variation of various different ranges and for the different values of the flow significant parameters. The outcomes of the problem are summarized as follows;

- For the increased values of the Permeability parameter (K), Grashof number (Gr), modified Grashof number (Gc) and Casson parameter (β) increase the velocity profiles, but the reverse trend is observed in magnetic parameter(M).
- The fluid velocity and temperature decreases when Prandtl number (Pr) increases.
- The Temperature level of the fluid decreases when the Heat source parameter (Q) and Radiation parameter (R) increases.
- Higher chemical reaction parameter (Kr) and Schmidt number (Sc) causes the numerous reductions in velocity and Concentration profiles.
- With the effect of Permeability parameter, radiation parameter and chemical reaction parameter is to increase the skin-friction coefficient whereas reverse trend is observed with the increase in magnetic parameter and the Nusselt number and Sherwood number increases with the increases of Radiation and Permeability parameter respectively.

APPENDIX

$$\begin{aligned}
m_1 &= \frac{Sc + \sqrt{Sc^2 + 4KrSc}}{2}, m_2 = \frac{Sc + \sqrt{Sc^2 + 4(Kr+n)Sc}}{2}, m_3 = \frac{Pr + \sqrt{Pr^2 + 4F_1}}{2}, F_1 = Q + R \\
m_4 &= \frac{Pr + \sqrt{Pr^2 + 4(F_1 + n)}}{2}, m_5 = \frac{1 + \sqrt{1 + 4\left(1 + \frac{1}{\beta}\right)N}}{2\left(1 + \frac{1}{\beta}\right)}, m_6 = \frac{1 + \sqrt{1 + 4\left(1 + \frac{1}{\beta}\right)(N+n)}}{2\left(1 + \frac{1}{\beta}\right)} \\
A_1 &= \frac{Am_1}{m_1^2 - Scm_1 - Sc(Kr+n)}, A_2 = 1 - A_1, A_3 = \frac{Am_3}{m_3^2 - Prm_3 - (F_1 + n)}, A_4 = 1 - A_3 \\
A_5 &= \frac{-Gr}{\left(1 + \frac{1}{\beta}\right)m_3^2 - m_3 - N}, A_6 = \frac{-Gc}{\left(1 + \frac{1}{\beta}\right)m_1^2 - m_1 - N}, A_7 = u_p - A_5 - A_6 - 1 \\
A_8 &= \frac{m_3AA_7}{\left(1 + \frac{1}{\beta}\right)m_3^2 - m_3 - (N+n)}, A_9 = \frac{m_3AA_5}{\left(1 + \frac{1}{\beta}\right)m_3^2 - m_3 - (N+n)}, A_{10} = \frac{m_1AA_6}{\left(1 + \frac{1}{\beta}\right)m_1^2 - m_1 - (N+n)} \\
A_{11} &= \frac{-GrA_4}{\left(1 + \frac{1}{\beta}\right)m_4^2 - m_4 - (N+n)}, A_{12} = \frac{-GrA_3}{\left(1 + \frac{1}{\beta}\right)m_1^2 - m_1 - (N+n)}, A_{13} = \frac{-GcA_2}{\left(1 + \frac{1}{\beta}\right)m_2^2 - m_2 - (N+n)} \\
A_{14} &= \frac{-GcA_1}{\left(1 + \frac{1}{\beta}\right)m_1^2 - m_1 - (N+n)}, A_{15} = A_9 + A_{12}, A_{16} = A_{10} + A_{14}, A_{17} = -(A_8 + A_{11} + A_{15} + A_{13} + A_{16})
\end{aligned}$$

References

- [1] S.A.Shehzad, and T. Hayat: Effects of mass transfer on MHD flow of Casson fluid with chemical reaction. Brazilian Journal of chemical Engineering, 30, 187-195, 2013.
- [2] Vajravelu, K., and Mukhopadhyay, S: Diffusion of chemically reactive species in Casson fluid flow over an unsteady permeable stretching surface, J. Hydrodyn. 25, 591-598, 2013.
- [3] Abid Hussanan, Mohd Zuki Salleh: Unsteady boundary layer flow and heat transfer of a Casson fluid past an oscillating vertical plate with Newtonian heating, PLoS One, v.9(10), 2014.
- [4] Sekhar Kuppala R Viswanatha Reddy G: Unsteady MHD convective heat and mass transfer of a Casson fluid past a semi-infinite vertical permeable moving plate with heat source/sink, Chemical and Process Engineering Research, Vol.39, 2015.
- [5] Animasaun, I.L: Effects of thermophoresis, variable viscosity and thermal conductivity on free convective heat and mass transfer of non-Darcian MHD dissipative Casson fluid flow with suction and nth order of chemical reaction. Journal of the Nigerian Mathematical Society, 34, 11-31, 2015.
- [6] B. Suresh, P. H. Veena, V. K. Pravin: Free convective heat transfer flow of a Casson fluid with radiative and dissipative effect due to variable thermal conductivity and internal heat generation past a stretching sheet, International Journal Of Engineering Sciences & Research Technology, 5(10), 638-654, 2016
- [7] B. O. Falodun, S. E. Fadugba: Effects of heat transfer on unsteady magnetohydrodynamics (MHD) boundary layer flow of an incompressible fluid a moving vertical plate, World Scientific News, 88(2), 118-137, 2017
- [8] B. O. Falodun: Magnetohydrodynamics (MHD) heat and mass transfer of Casson fluid flow past a semi-infinite vertical plate with thermophoresis effect: spectral relaxation analysis, Defect and Diffusion Forum, Vol. 389, pp. 18-35, 2018
- [9] Y. Hari Krishna, G.V. Ramana Reddy and O.D. Makinde: Chemical reaction effect on MHD flow of Casson fluid with porous stretching sheet, Defect and Diffusion Forum, Vol. 389, pp. 100-109, 2018
- [10] P. Rama Krishna Reddy, M. C. Raju: MHD free convective flow past a porous plate, International Journal of Pure and Applied Mathematics, 118(5), 507-529, 2018.
- [11] P. Nagasantoshi, G. V. Ramana Reddy, M. Gnaneswara Reddy, and P. Padma: Heat and mass transfer of non-Newtonian nanofluid flow over a stretching sheet with non-uniform heat source and variable viscosity, J. Nanofluids, 7(5), 821-832, 2018.
- [12] Reddy, GV Ramana; Krishna, Y Hari; Soret and Dufour Effects on MHD Micropolar Fluid Flow Over a Linearly Stretching Sheet, Through a Non-Darcy Porous Medium, International Journal of Applied Mechanics and Engineering, 23(2), 485-502, 2018.
- [13] Suneetha, K; Ibrahim, SM; Reddy, GV Ramana Reddy: Radiation and heat source effects on MHD flow over a permeable stretching sheet through porous stratum with chemical reaction, Multidiscipline Modeling in Materials and Structures, 14(5), 1101-1114, 2018.
- [14] Vijaya, N; Hari Krishna, Y; Kalyani, K; Reddy, GVR; Soret and radiation effects on an unsteady flow of a Casson fluid through porous vertical channel with expansion and contraction, Frontiers in Heat and Mass Transfer, 11, 2018.
- [15] Reddy, G; Krishna, Y Hari; Numerical solutions of unsteady MHD flow heat transfer over a stretching surface with suction or injection FDMP-Fluid Dynamics & Materials Processing, 14(3), 213-222, 2018.

ISSN 1584 - 2665 (printed version); ISSN 2601 - 2332 (online); ISSN-L 1584 - 2665

copyright © University POLITEHNICA Timisoara, Faculty of Engineering Hunedoara,
5, Revolutiei, 331128, Hunedoara, ROMANIA<http://annals.fih.upt.ro>